Fluid Solution and Solid-State Electron Nuclear Double Resonance Studies of Flavin Model Compounds and Flavoenzymes

H. Kurreck,* M. Bock, N. Bretz, M. Elsner, H. Kraus, W. Lubitz, F. Müller,[1] J. Geissler,[2] and P. M. H. Kroneck[2]

Contribution from the Institut für Organische Chemie, Freie Universität Berlin, 1000 Berlin 33, West Germany. *Received July 21, 1983*

Abstract: Partially deuterated and various substituted flavin and thiaflavin model compounds have been synthesized. For the first time, high-resolution H, D, and ^{14}N ENDOR and TRIPLE resonance experiments in fluid solutions have been performed on the paramagnetic derivatives of these compounds. Additionally, valuable information has been obtained about hyperfine anisotropies and molecular structures from ENDOR in rigid matrices. Solid matrix ENDOR studies of native flavoenzymes, namely, "Old Yellow Enzyme" (NADPH dehydrogenase), two flavodoxins, and a methanol oxidase are reported. The ENDOR matrix signals of the various flavoproteins are different in intensity, suggesting that the microenvironments are remarkably different. Applicabilities and limitations of the ENDOR technique in the studies of flavins and flavoenzymes are discussed.

Flavins are known to be ubiquitous redox cofactors in all biological redox chains. The roles and occurrence of flavoproteins in biological systems have exhaustively been discussed in a variety of authoritative review articles, e.g., ref 3. Thus, here we confine ourselves to a short description of those properties of the flavins which we believe to be relevant in the context of this investigation. The prosthetic groups of the flavoenzymes are riboflavin (vitamin B_2), flavin mononucleotide (FMN), and flavin adenine dinucleotide (FAD) (see Figure 1). Lumiflavin, which is widely used as a flavin model compound, carries a methyl group at N(10) instead of the ribityl side chain. The redox active site of these cofactors is the isoalloxazine system, which can occur in three different reversible oxidation steps, i.e., quinoid (oxidized), semiquinoid (radical), and hydroquinoid (1,5-dihydro) state. This enables flavins to mediate between two-electron and one-electron transfer processes. It is believed that the mode of the reaction of flavin is regulated by the apoprotein. According to this hypothesis, regulation of the mechanism is brought about by positive charges or hydrogen bridges from the protein to either the N(1) or the N(5) site of the flavin molecule.[3b,4] This mechanism results in "blocking" and "deblocking" of the N(1) and N(5) position, respectively. Concomitantly, the radical state is stabilized (one-electron transfer is favored) or destabilized (two-electron transfer is favored). In order to obtain further insight in the reaction mode of these "redox shuttles", some "mutilated" flavin type systems have been studied as (anti) metabolites, namely, 5-thia-5-deazaflavins and 5-deazaflavins.[5] Whereas the former flavin analogue lacks reversible two-electron transfer capability, the latter is known to suppress strictly one-electron activities.

The flavin radicals can occur in different protonation states, i.e., cation, neutral, and anion radical.[3g] In the investigation of the model compounds, the protonation state present in the sample under study is dependent on the pH of the solution, whereas in the flavoenzymes formation of the anion or neutral radical state is determined by the type of binding and interaction of the prosthetic group to the apoprotein.[4b] In biological systems cation radicals cannot occur because the acidic conditions required would lead to denaturation of the proteins. In the studies of the paramagnetic species of flavins, application of ESR spectroscopy has yielded valuable information on the structures and properties of these radicals. The ENDOR technique has also been applied to flavin systems.[6] Its much higher resolving power compared to that of conventional ESR makes this technique very attractive in studies of such complex radical species.

The theory of proton and non-proton ENDOR is covered by several papers published in the literature, e.g., ref 7. For a better understanding of the results of this contribution, the following facts valid for a *doublet spin system* are briefly summarized.

(a) Each set of equivalent hyperfine coupled nuclei—no matter how many nuclei belong to this set—gives rise to one pair of ENDOR lines. The number of ENDOR lines increases only additively with the number of different sets of nuclei. These facts explain the above-mentioned resolution enhancement of ENDOR as compared to that of ESR where the number of lines increases geometrically with the number of different sets of nuclei.

(b) According to the ENDOR resonance condition

$$\nu_{ENDOR} = |\nu_n \pm A/2|$$

the ENDOR line pair may either be centered around the free nuclear frequency and spaced by the hyperfine coupling constant ($A/2 < \nu_n$) or may be centered around half the hyperfine coupling constant and spaced by twice the free nuclear frequency ($A/2 > \nu_n$). The former condition normally holds for the protons whereas the latter very often is valid for non-proton nuclei with smaller magnetic moments, e.g., nitrogen.

(c) Different types of nuclei often require quite different experimental conditions, such as temperature, microwave power, and rf power levels. Typically, proton ENDOR lines occur at

(1) Department of Biochemistry, Agricultural University 11, De Dreijen, 6703 BC Wageningen, The Netherlands.

(2) Fakultät für Biologie, Universität Konstanz, 7750 Konstanz, West Germany.

(3) (a) Massey, V.; Gibson, Q. H. *Fed. Proc., Fed. Am. Soc. Exp. Biol.* **1964**, *23*, 18. (b) Hemmerich, P.; Massey, V.; Michel, H.; Schug, Ch. *Struct. Bonding (Berlin)* **1982**, *48*, 93. Müller, F. *Top. Curr. Chem.* **1983**, *108*, 71. (c) Hemmerich, P. *Proc. R. Soc. London, Ser. A.* **1968**, *302*, 335. (d) Beinert, H.; Sands, R. H. "Free Radicals in Biological Systems"; Academic Press: New York, 1961; p 17. (e) Penzer, G. R.; Radda, G. K. *Q. Rev., Chem. Soc.* **1967**, *21*, 43. (f) Hemmerich, P. *Adv. Chem. Ser.* **1977**, *No. 162*, 311. (g) Hemmerich, P. *Fortschr. Chem. Org. Naturst.* **1976**, *33*, 451. (h) Edmondson, D. E. "Biological Magnetic Resonance"; Plenum Press: New York, 1978; Vol. 1, p 205f.

(4) (a) Müller, F. *Z. Naturforsch., B: Anorg. Chem., Org. Chem., Biochem., Biophys., Biol.* **1972**, *27B*, 1058. (b) Müller, F.; Hemmerich, P.; Ehrenberg, A.; Palmer, G.; Massey, V. *Eur. J. Biochem.* **1970**, *14*, 185.

(5) (a) Duchstein, H. J.; Fenner, H.; Hemmerich, P.; Knappe, W. R. *Eur. J. Biochem.* **1979**, *95*, 167. (b) Fenner, H.; Grauert, R.; Hemmerich, P.; Michel, H.; Massey, V. *Eur. J. Biochem.* **1979**, *95*, 183.

(6) See, e.g.: (a) Fritz, J.; Müller, F.; Mayhew, S. B. *Helv. Chim. Acta* **1973**, *56*, 2250. (b) Eriksson, L. E. G.; Ehrenberg, A. *Biochim. Biophys. Acta* **1973**, *293*, 57. (c) Ehrenberg, A.; Eriksson, L. E. G.; Hyde, J. S. *Biochim. Biophys. Acta* **1968**, *167*, 482. (d) Eriksson, L. E. G.; Ehrenberg, A.; Hyde, J. S. *Eur. J. Biochem.* **1970**, *17*, 539. (e) Eriksson, L. E. G.; Hyde, J. S.; Ehrenberg, A. *Biochim. Biophys. Acta* **1969**, *192*, 211. (f) Salach, J.; Walker, W. H.; Singer, T. P.; Ehrenberg, A.; Hemmerich, P.; Ghisla, S.; Hartmann, U. *Eur. J. Biochem.* **1972**, *26*, 267.

(7) (a) Möbius, K.; Plato, M.; Lubitz, W. *Phys. Rep.* **1982**, *87*, 172. (b) Dorio, M. M.; Freed, J. H.; Eds. "Multiple Electron Resonance Spectroscopy"; Plenum Press: New York, 1979. (c) Kevan, L.; Kispert, L. D. "Electron Spin Double Resonance Spectroscopy"; Wiley: New York, 1976. (d) Plato, M.; Lubitz, W.; Möbius, K. *J. Phys. Chem.* **1981**, *85*, 1202. (e) Kirste, B.; Kurreck, H.; Lubitz, W.; Zimmermann, H. *J. Am. Chem. Soc.* **1980**, *102*, 817.

0002-7863/84/1506-0737$01.50/0

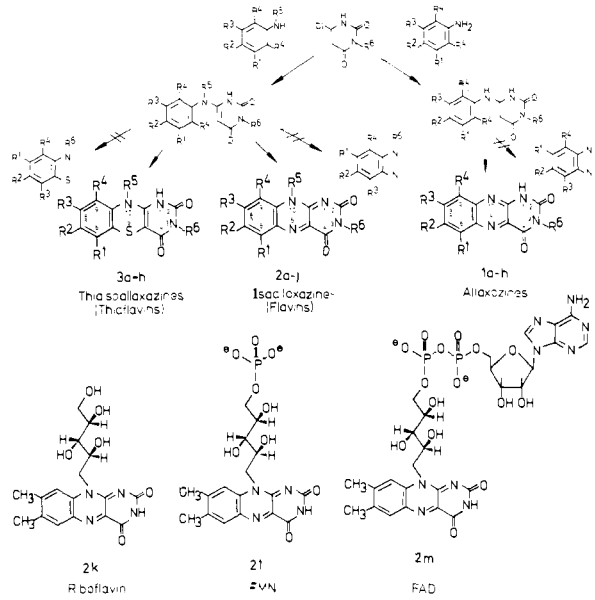

Figure 1. Reaction scheme and structures of compounds. The numbers of the radicals refer to the differently protonated molecules, e.g., $\mathbf{2a}^{+\cdot}$ denotes the 2-fold protonated radical cation of **2a**.

lower temperatures as compared to the optimum ENDOR conditions of, e.g., nitrogen ENDOR resonances.

(d) ENDOR experiments can, in principle, be performed in isotropic fluid solutions, in rigid matrices, or in liquid crystals. In fluid solution high resolution is obtained at the expense of loss of information about the anisotropic interactions, i.e., only the isotropic hyperfine coupling constants are accessible. In solid matrices, neglecting single-crystal studies, anisotropic broadening very often prevents detection of the ENDOR signals. Only in favorable cases, e.g., for the protons of freely rotating methyl groups, can prominent ENDOR lines be obtained. On the other hand, ENDOR in solid media is a powerful tool for probing the surroundings of the magnetic nuclei under study (see, e.g., the discussion of the free nuclear frequency MATRIX ENDOR signals, vide infra).

(e) Extension of ENDOR to general electron nuclear triple (general TRIPLE) resonance allows determination of the relative signs of the hyperfine coupling constants. In a general TRIPLE experiment a second saturating rf field is applied to one transition, causing significant changes in the intensity ratios of the high-/low-frequency ENDOR signals, cf. Figure 4. The relative signs of the couplings can be deduced from the amplitude changes. A detailed description of this technique is given in ref 7a,b.

(f) In "special TRIPLE" the high- and low-frequency transitions belonging to one set of nuclei are driven simultaneously, resulting in only *one* special TRIPLE signal occurring at $a_i/2$. For more details, see ref 7a. In special TRIPLE, often a better signal to noise ratio and resolution are obtained as compared to those in ENDOR.

The model compound studies of this paper focus on ENDOR investigations of the paramagnetic state of the flavins. In addition, we include some preliminary results of our studies on the paramagnetic thiaflavin analogues; solid-state ENDOR studies of the flavoenzymes NADPH dehydrogenase from brewer's yeast ("Old Yellow enzyme"), flavodoxins from *Azotobacter vinelandii* and *Megasphaera elsdenii*, and a methanol-utilizing enzyme (methanol oxidase) are reported.

Experimental Section

Instrumentation. The mass spectra were recorded on a CH 5-DF Varian-MAT spectrometer. The NMR spectra were recorded on a Bruker WH 270 or on a Varian XL 100 with tetramethylsilane as the internal standard.

The spectrometer used for ESR, ENDOR, and TRIPLE basically consists of a Bruker ER 220 D ESR spectrometer equipped with a Bruker cavity (ER 200 ENB) and home-built NMR facilities described elsewhere.[8] ENDOR spectra were accumulated by using a Nicolet Averager 1170 employing 1K data points; typically 32, 64, or 128 sweeps were taken, 30 s/scan, time constant 40 ms. The temperature (±1 K) was varied with a Bruker B-VT temperature control unit and checked by means of a thermocouple: for fluid solutions, 260–310 K [$B_{NMR} \approx$ 0.4–0.5 mT (14 MHz) in the rotating frame, microwave power 200 mW (radicals of isoalloxazines and alloxazines); $B_{NMR} \approx$ 0.4–0.5 mT (14 MHz), 30–40 mW (thiaisoalloxazine radicals); FM of the NMR field (10 kHz), amplitude 70 kHz]; for disordered solids, 110–150 K [$B_{NMR} \approx$ 0.4–0.5 mT (14 MHz), microwave power 20–25 mW; FM of the NMR field (10 kHz), amplitude 80–100 kHz].

Preparation of Model Compounds. Alloxazines, isoalloxazines, and thiaisoalloxazines were synthesized following the procedures given in the literature,[9,10] i.e., by reacting the appropriately substituted anilines with 6-chloro-3-methyluracil[11] to obtain the 6-anilino-3-methyluracils. Subsequent ring closure with sodium nitrite and reduction with sodium dithionite or thionyl chloride followed by reduction with thiophenol, respectively, yielded the desired molecules (see the reaction scheme, Figure 1). As can be seen from Figure 1 this ring closure reaction can, in principle, occur in two different ways, resulting in the formation of isomers if the anilines are unsymmetrically (methyl) substituted ($R^1 \neq R^3$) and $R^4 = H$. For example, the starting material (3-methylanilino)uracil ($R^3 = CH_3$; $R^1 = R^2 = R^4 = H$) could lead to 8-methylisoalloxazine or 8-methylthiaisoalloxazine ($R^3 = CH_3$) and to 6-methylisoalloxazine or 6-methylthiaisoalloxazine ($R^1 = CH_3$). Since the NMR spectrum of the isoalloxazine derivative shows only one ortho coupling of 8–9 Hz (H-6, H-7), the *exclusive* formation of the (desired) 8-methyl isomer can safely be assumed. In the case of the thiaisoalloxazine, however, small amounts of the undesired isomer could be detected in the NMR spectra (two ortho couplings: H-7, H-8; H-8, H-9). The latter could be removed by recrystallization. Alkylation of the isoalloxazines in position 3 was performed as described.[12] The structures of the alloxazines, isoalloxazines, and thiaisoalloxazines were deduced unambiguously from elemental analysis, combined with standard spectroscopic techniques (Table I). In the following, only new compounds are described including those mentioned in the literature without a detailed report of the analytical data.

Anilines. N,3,4-trimethylbenzenamine and 3,4-dimethyl-*N*-(trideuteriomethyl)benzenamine were synthesized as described in the literature.[13] The aniline analogue deuterated in positions 2 and 6 was obtained as the deuteriochloride by refluxing the hydrochloride of the undeuterated precursor in deuterium oxide. Deuteration of position 5, to yield the deuteriochloride of *N,N*,2,5,6-Pentadeuterio-3,4-dimethylbenzenamine, was achieved by treating the precursor in a sealed tube with concentrated deuterium chloride at 250 °C twice for 12 h.

Deuterated 6-Anilino-3-methyluracils. The synthesis of the deuterated 6-anilino-3-methyluracils from the deuterated benzenamines and 6-chloro-3-methyluracil required a different condition than that of the unlabeled compounds because the published synthetic route yielded a loss of 15% of the deuterium. When the deuterated benzenamine derivatives were heated with the sodium salt of 6-chloro-3-methyluracil in tri-*n*-butylamine at 160 °C for 5 min the deuterated 6-anilino-3-methyluracils were obtained (95% deuterium).

In Table II the analytical data of the anilinouracils are given.

8α-Morpholinotetraacetylriboflavin. Tetraacetylriboflavin was monobromated in position 8α and the reaction mixture separated by HPLC (57% yield of the 8α-bromotetraacetylriboflavin). Subsequent heating with morpholine followed by chromatography over Dowex resin yielded 8α-morpholinotetraacetylriboflavin in very poor yield.[14]

NADPH Dehydrogenase [NADPH: (Acceptor) Oxidoreductase, EC 1.6.99.1]. Old Yellow enzyme (OYE) was isolated from dried brewer's bottom yeast according to the affinity column procedure developed by Abramowitz and Massey.[15] Subsequently the pure solution of the enzyme was concentrated by ultrafiltration and stored at −25 °C after rapid freezing. The turnover number, measuring the number of NADPH molecules oxidized per second per molecule of enzyme-bound FMN, was determined by the following standard procedure. First, 1.3 nmol of NADPH dehydrogenase and 240 nmol of NADPH are dissolved in 1.5

(8) (a) Fey, H. J.; Kurreck, H.; Lubitz, W. *Tetrahedron* **1979**, *35*, 905. (b) Kurreck, H.; Kirste, B.; Lubitz, W. *Angew. Chem.*, in press.
(9) Yoneda, F.; Sakuma, Y.; Shinanna, K. *J. Am. Chem. Soc.* **1976**, *98*, 830.
(10) Fenner, H.; Grauert, R. W.; Tessendorf, L. *Arch. Pharm. (Weinheim, Ger.)* **1981**, *314*, 874.
(11) Nübel, G.; Pfleiderer, W. *Chem. Ber.* **1962**, *95*, 1605.
(12) Hemmerich, P.; Prijs, B.; Erlenmeyer, H. *Helv. Chim. Acta* **1960**, *43*, 372.
(13) Pailer, M.; Hübsch, W. J. *Monatsh. Chem.* **1966**, *97*, 1541. Johnstone, R. A. W.; Payling, D. W.; Thomas, C. *J. Chem. Soc. C* **1969**, *16*, 223.
(14) Walker, W. H.; Singer, T. P.; Ghisla, S.; Hemmerich, P. *Eur. J. Biochem.* **1972**, *26*, 279.
(15) Abramowitz, A. G.; Massey, V. *J. Biol. Chem.* **1976**, *251*, 5321.

Table I. Numbering of Compounds and Analytical Data

compd no.	R^1	R^2	R^3	R^4	R^5	R^6	mp, °C	M^+	yield, %	C, calcd, exptl	H, calcd, exptl	N, calcd, exptl	S, calcd, exptl
1a	H	H	H	H	H	H							
1b	H	H	CH_3	H	H	CH_3	329	242	85	59.50, 59.33	4.16, 4.22	23.13, 23.03	
1c	H	CH_3	H	H	H	CH_3	299	242	63	59.50, 59.51	4.16, 4.24	23.13, 23.21	
1d	CH_3	H	CH_3	H	H	CH_3	295-298	256	82	60.93, 61.00	4.72, 4.70	21.86, 22.01	
1e	H	CH_3	CH_3	H	H	H							
1f	H	CH_3	CH_3	H	H	CH_3							
1g	H	CH_3	CH_3	D	H	CH_3	318-322	257	41				
1h	D	CH_3	CH_3	D	H	CH_3	319-325	258	20				
2a[f]	H	H	H	H	CH_3	CH_3							
2b[f]	H	H	CH_3	H	CH_3	CH_3	281-284	256	80				
2c[f]	H	CH_3	H	H	CH_3	CH_3	285-288	256	59	60.93, 60.42	4.72, 4.71	21.86, 21.99	
2d	CH_3	H	CH_3	H	CH_3	CH_3	313-315	270	90	62.21, 61.39	5.22, 5.14	20.73, 20.75	
2e	H	CH_3	CH_3	H	CH_3	H							
2f	H	CH_3	CH_3	H	CH_3	CH_3							
2g	H	CH_3	CH_3	D	CH_3	CH_3	283-286	271	37				
2h	D	CH_3	CH_3	D	CH_3	CH_3	281-285	272	42				
2i	H	CH_3	CH_3	H	CD_3	CH_3	282-285	273	51				
2j	H	CH_3	CH_3	H	CH_3	CD_3	278-281	273	92				
2k[a]	H	CH_3	CH_3	H		H							
2l[b]	H	CH_3	CH_3	H		H							
2m[c]	H	CH_3	CH_3	H		H							
2n	H	CH_3	CH_3	H	CH_3	$CH_2COOC_2H_5$							
2o[d]	H	CH_3		H		H							
2p[e]	H	CH_3	CH_3	H		H							
3a[g]	H	H	H	H	CH_3	CH_3							
3b	H	H	CH_3	H	CH_3	CH_3	298	275	51				
3c	H	CH_3	H	H	CH_3	CH_3	308-310	275	89	56.71, 56.51	4.76, 4.77	15.26, 15.02	11.08, 10.84
3d	CH_3	H	CH_3	H	CH_3	CH_3	320-325	289	92	58.12, 57.91	5.23, 5.21	14.52, 14.65	
3e	H	CH_3	CH_3	H	CH_3	CH_3							
3f	H	CH_3	CH_3	D	CH_3	CH_3	315-326	290	22				
3g	D	CH_3	CH_3	D	CH_3	CH_3		291	5				
3h[g]	H	H	H	H	H	CH_3							

[a] R^5 = D-ribityl. [b] R^5 = D-ribityl phosphate. [c] R^5 = adenosyl-D-ribityl phosphate. [d] R^4 = 8α-morpholino; R^5 = tetraacetyl-D-ribityl. [e] R^5 = tetraacetyl-D-ribityl. [f] See ref 29. [g] See ref 22.

Table II Analytical Data of Anilinouracils

-6-(phenylamino)-2,4-(1*H*,3*H*)-pyrimidinedione	mp, °C	yield, %	C_{calcd}	C_{found}	H_{calcd}	H_{found}	N_{calcd}	N_{found}
3,3'-$(CH_3)_2$	259-261	68	62.33	62.40	5.67	5.71	18.17	18.14
3,4'-$(CH_3)_2$	290-293	70	62.33	62.38	5.67	5.69	18.17	18.17
3,3',5'-$(CH_3)_3$	275-277	66	63.66	63.83	6.16	6.17	17.13	17.09
3,3',*N'*-$(CH_3)_3$	186-187	69	63.66	63.65	6.16	6.13	17.13	17.32
3,4',*N'*-$(CH_3)_3$	238-240	65	63.66	64.04	6.16	6.16	17.13	17.21
3,3',5',*N'*-$(CH_3)_4$	183-184	55	64.85	64.45	6.61	6.62	16.21	16.04
3,3'-$(CH_3)_3$-2',6'-d_2		28[a]						
3,3',4'$(CH_3)_3$-2',5',6'-d_3		20[a]						
3,3',4',*N'*-$(CH_3)_4$-2',6'-d_2		35[a]						
3,3',4',*N'*-$(CH_3)_4$-2',5',6'-d_3		37[a]						
3,3',4'-$(CH_3)_3$,*N'*-(CD_3)		40[a]						

[a] These compounds were used without further purification.

mL 0.1 M KP_i buffer (pH 7). Then at 20 °C the rate of pyridine nucleotide oxidation was determined by UV spectroscopy observing the absorption at 340 nm, yielding a turnover number of 0.54 [mol of NADPH (mol of FMN)$^{-1}$ s^{-1}]. Within experimental error the same value was obtained before and after the ENDOR measurements, indicating that the enzyme activity is not affected by these experiments.

Flavodoxins from *M. elsdenii* and *A. vinelandii*. The flavodoxins were prepared as described previously.[16] The pure proteins were freeze-dried and stored at −25 °C.

Methanol Oxidase (Alcohol:Oxygen Oxidoreductase, EC 1.1.3.13). The enzyme was isolated from the yeast *Candida boidinii* following the procedure given by Sahm and Wagner.[17] The purified enzyme was frozen immediately after preparation and stored at −25 °C.

Analytical Methods. Protein concentrations were determined by the methods of Lowry et al.[18] and Bradford.[19] The purity of the proteins was checked by sodium dodecyl sulfate gel electrophoresis.[20] Essentially the same data were obtained as described in the literature.

Generation of the Radicals. The radicals for ENDOR in solution were generated on a high-vacuum line by using standard techniques (see, e.g., ref 8b). Samples for solid-state ENDOR were prepared in quartz tubes.

Cation Radicals. Fluid solutions of the alloxazine and isoalloxazine cation radicals were obtained in CF_3COOH/toluene mixtures with $Na_2S_2O_4$ or Zn as the reducing agent.[21] Solutions of the radicals in HCl, DCl, CF_3COOH/toluene, CF_3COOD/toluene, or CCl_3COOH/toluene were frozen for solid-state measurements after Zn reduction of the respective precursors. Thiaisoalloxazine cation radicals were obtained in CF_3COOH/toluene or in HCl by oxidizing the diamagnetic precursors with dibenzoyl peroxide.[22]

Neutral Radicals. A solution of 3-ethoxyacetoisoalloxazine or tetraacetylriboflavin in CH_2Cl_2 or $CHCl_3$ was reduced by an aqueous solution of $Na_2S_2O_4$ either to the semiquinone state (only stable in frozen solution) or to the dihydro state. To obtain the stable neutral radical the dihydroflavins were methylated with CH_3I in CH_2Cl_2 or $CHCl_3$ in the presence of triethylamine. Reoxidation of the thus obtained N^5-methyl-1,5-dihydroflavins by I_2 or O_2 gave the stable radicals, which were transferred to a vacuum line, made anaerobic, and studied in a sealed

(16) Mayhew, S. G.; Massey, V. *J. Biol. Chem.* **1969**, *244*, 794. Hinkson, J. W.; Buten, W. A. *J. Biol. Chem.* **1967**, *242*, 3345.
(17) Sahm, H.; Wagner, F. *Eur. J. Biochem.* **1973**, *36*, 250.
(18) Lowry, D.; Rosebrough, N.; Farr, A.; Randall, R. *J. Biol. Chem.* **1951**, *193*, 265.
(19) Bradford, M. *Anal. Biochem.* **1976**, *72*, 248.
(20) King, J.; Laemmli, U. K. *J. Mol. Biol.* **1971**, *62*, 465.
(21) Walker, W. H.; Ehrenberg, A. *FEBS Lett.* **1969**, *3*, 315.
(22) Grauert, R. W. Thesis, Freie Universität Berlin, 1976.

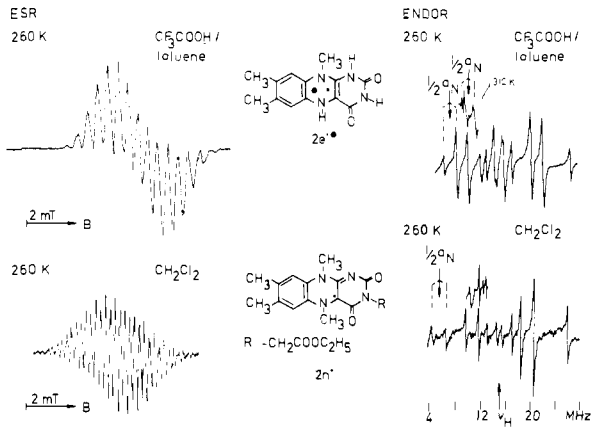

Figure 2. ESR and ENDOR spectra of the lumiflavin cation radical (top) and neutral radical of the 3-ethoxyaceto derivative of lumiflavin.

tube.[4b,23] Neutral thiaisoalloxazine radicals were obtained in $CHCl_3$ by dissolving the respective dimer, which was synthesized as described previously.[5b]

Anion Radicals. 3-Ethoxyacetoisoalloxazine was treated with phenylmagnesium bromide or with *n*-butyllithium in tetrahydrofuran. FMN and FAD anion radicals were generated in aqueous NaOH (0.001 N) by using $Na_2S_2O_4$ as the reducing agent.

Radical States of the Enzymes. A solution of 0.5 mM NADPH dehydrogenase and 10 mM EDTA in 20 mM Tris buffer, pH 9, was carefully made anaerobic by repeatedly removing the air (vacuum pump) and exchanging it for purified nitrogen. Subsequently the solution was illuminated until the maximum amount of radical had formed (two slide projectors (250 W) were used).[24]

The solutions of the flavodoxins in 0.1 M KP_i buffer, pH 7, were made anaerobic and mixed with a solution of $Na_2S_2O_4$. For *M. elsdenii* flavodoxin 1 redox equiv and for *A. vinelandii* flavodoxin 1.2–2.0 redox equiv of a $S_2O_4^{2-}$ solution were used.[16,25] The color changed from yellow to deep blue, indicating the generation of the radical.

Methanol oxidase in 30 mM KP_i buffer, pH 7, was made anaerobic and used directly for the ESR and ENDOR studies. Addition of 1 mM NH_2OH results in a 2.5-fold increase of the radical concentration.[26]

Results

Fluid Solution Measurements of Model Compounds.[27] Figure 2 shows the high resolution ESR and ENDOR spectra of the lumiflavin cation radical (**2e**$^{+}$·) in trifluoroacetic acid/toluene and of a derivative of the lumiflavin neutral radical **2n**· in methylene chloride. From the ENDOR spectrum of **2e**$^{+}$· six proton and two nitrogen hyperfine coupling constants (hfsc's) could be deduced. An improved ENDOR response of the larger N ENDOR signal occurred at higher temperatures, indicating the larger hyperfine anisotropy of this position.[6b] The ENDOR spectrum of the neutral radical shows five proton and two nitrogen hfsc's, the values of which are quite different from those of **2e**$^{+}$· (see Table III). Relative signs of the hfsc's could be obtained from general TRIPLE measurements. Since the ENDOR line intensities do not reflect the number of nuclei belonging to the different sets of nuclei[28] assignments of the hfsc's to molecular positions were only possible by using selectively deuterated derivatives. Figure 3 shows the ENDOR spectra of differently deuterated isoalloxazine cation radicals. In addition to the H and N ENDOR lines, D ENDOR resonances could be obtained when the protons at N(1) and N(5) were exchanged with deuterons by using deuterated trifluoroacetic acid as a solvent. As expected, the largest H hfsc [N(5)H] no longer shows up in this experiment.

Figure 4 depicts the ENDOR and general TRIPLE spectra of thiaisoalloxazine cation radical **3e**$^{+}$·. Five sets of H ENDOR

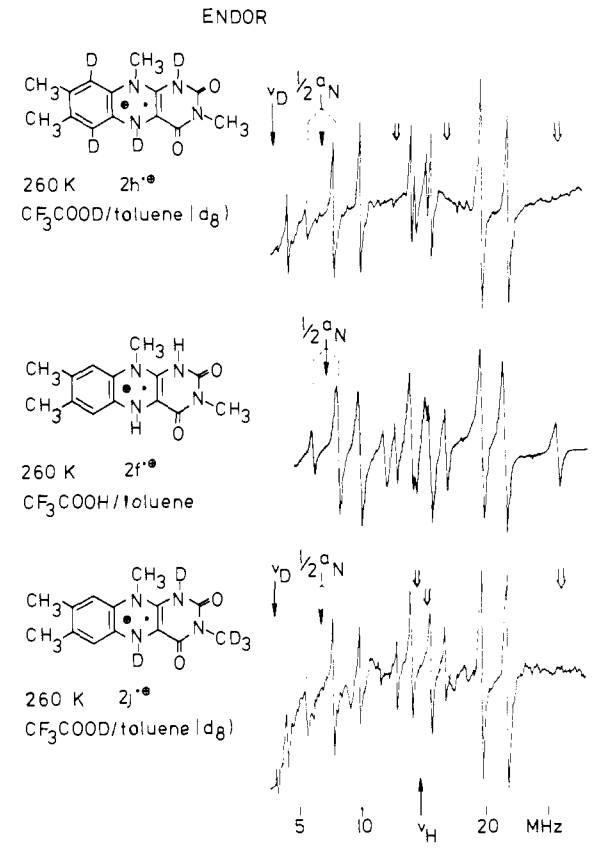

Figure 3. ENDOR spectra of the 3-methyllumiflavin cation radical and two selectively deuterated derivatives. The arrows indicate the ENDOR frequency positions of the exchanged protons.

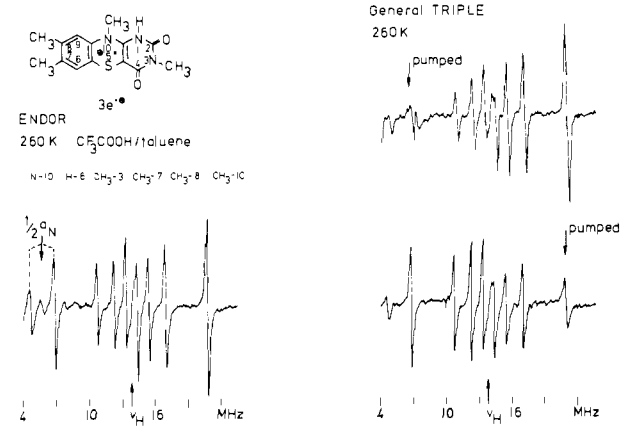

Figure 4. ENDOR (left) and general TRIPLE spectra of the thiaisoalloxazine cation radical **3e**$^{+}$·: B_{NMR} (scan) = 0.4 mT (14 MHz); B_{NMR}(pump) = 0.4 mT.

signals and one N ENDOR line pair could be obtained. In the thiaisoalloxazine series not only the cation but also the neutral radicals can easily be generated, the ESR and ENDOR spectra being comparable in signal to noise ratio and line width to those of the cations. Again assignments of the hfsc's to molecular positions could be achieved by using selectively deuterated derivatives (see Table III).

Solid-State ENDOR Measurements of Model Compounds. In isotropic fluid solution Brownian motion causes averaging of the static part of the anisotropic hyperfine interaction and—as was shown in the previous section—often well-resolved ESR and ENDOR spectra with narrow lines can be obtained. Freezing of the solution results in the formation of a glassy or polycrystalline (or amorphous) matrix. Hence, anisotropic broadening of the resonance signals significantly decreases the spectral resolution.[7c] The most pronounced ENDOR signals obtained from experiments in disordered solids are, in fact, the MATRIX ENDOR line and

(23) Ghisla, S.; Hartmann, K.; Hemmerich, P.; Müller, F. *Justus Liebigs Ann. Chem.* **1973**, 1388.
(24) Massey, V.; Palmer, G. *Biochemistry* **1966**, *5*, 3183.
(25) Edmondson, D. E.; Tollin, G. *Biochemistry* **1971**, *10*, 133.
(26) Geissler, J.; Hemmerich, P. *FEBS Lett.* **1981**, *126*, 152.
(27) Published in part in a preliminary communication: Bock, M.; Lubitz, W.; Kurreck, H.; Fenner, H.; Grauert, R. *J. Am. Chem. Soc.* **1981**, *103* (5), 5567.
(28) Dinse, K. P.; Biehl, R.; Möbius, K. *J. Chem. Phys.* **1974**, *61*, 4335.

Table III. Isotropic Hyperfine Coupling Constants (MHz)[a] in Fluid Solutions

compd no.	$a^{H}(3)$	$a^{N}(5)$	$a^{H}(5)$	$a^{H_\alpha}(6)$	$a^{H_s}(6)$	$a^{H_\alpha}(7)$	$a^{H_s}(7)$	$a^{H_\alpha}(8)$	$a^{H_s}(8)$	$a^{N}(10)$	$a^{H_\alpha}(10)$	$a^{H_s}(10)$
$1a^{+\cdot}$		21.46	23.62	4.13		1.27		7.43		11.23	12.07	
$1b^{+\cdot}$	1.23	21.44	−23.43	−4.03		2.09			+8.92	11.07	−11.94	
$1c^{+\cdot}$		21.01	22.75	3.30			1.87	7.64		11.41	11.95	
$1d^{+\cdot}$	+1.18	21.33	22.82		+1.85	−2.14			+8.75	11.21	−12.25	
$1e^{+\cdot}$	−1.25	21.22	−23.18	−3.31			+2.35		+9.36	11.06	−11.93	
$1g^{+\cdot}$	1.25	20.99	3.70[b]	3.30			2.33		9.20	11.05	2.00[b]	
$1h^{+\cdot}$	1.29		3.70[b]				2.34		9.10	11.05	2.00[b]	
$2a^{+\cdot}$		20.66	−23.06	−4.81		−0.90		−7.79		13.47		+14.09
$2b^{+\cdot}$	+0.86	21.00	−23.26	−4.75		−1.43			+9.54	13.10		+13.88
$2c^{+\cdot}$	0.98	20.32	22.71	−4.13			+1.46	−8.64		13.78		+14.18
$2d^{+\cdot}$	0.83	20.66	−22.06		+2.48	−1.32			+8.88	13.42		14.22
$2e^{+\cdot}$	0.90	20.73	−22.70	−4.03			+1.53		+9.95	13.19		+13.82
$2g^{+\cdot}$	0.90		3.68[b]	3.97			1.65		9.90	13.32		14.07
$2h^{+\cdot}$	0.90		3.63[b]				1.64		9.84	13.34		14.04
$2i^{+\cdot}$	0.88	22.56	3.56[b]	3.86			1.58		9.88	13.20		2.00[b]
$2j^{+\cdot}$			3.73[b]	3.96			1.60		9.88	13.40		14.04
$2k^{+\cdot}$	−0.80	+21.16	−23.30	−4.07			+1.53		+10.35	13.00		+7.33
$2l^{+\cdot}$	0.86	22.58	22.22	3.94			1.61		10.22	12.76		7.44
$2m^{+\cdot}$	0.79	21.09	22.86	3.96			1.61		10.27	12.88		7.49/6.91
2n·		22.08	+21.82[c]	−3.98			+0.83		+6.81	9.96		+11.02
2p·			22.35	3.92			0.86		6.70	8.70		6.70
$3a^{+\cdot}$	+0.97					−1.81		−4.30		13.07		+14.14
3a·	0.56					1.94		3.38		9.58		11.12
$3b^{+\cdot}$	1.02					−1.82			+5.78	13.14		+14.29
$3c^{+\cdot}$	+1.06						+2.80	−4.88		13.34		+14.32
$3d^{+\cdot}$	+0.98				−0.36	−2.78			+6.17	12.80		+13.90
3d·	1.31				0.18	1.84			4.24	9.60		11.49
$3e^{+\cdot}$	+1.06			0.32			+3.18		+6.30	13.08		+14.06
3e·	0.87			0.27			1.78		4.29	10.04		11.67
$3g^{+\cdot}$	1.00						3.12		6.10	13.10		14.14
$3h^{+\cdot}$	−1.23			−0.39		−2.72		−3.86		10.90	−11.79	

[a] All hfsc's are measured by ENDOR and are accurate within ±0.02 MHz (H) and ±0.03 MHz (N). Solvent: $CF_3COOH(D)$/toluene (cation radicals) or CH_2Cl_2 or $CHCl_3$ (neutral radicals). Temperature range 260–310 K. [b] Deuterium hfsc. [c] Methyl proton hfsc of CH_3 in position 5.

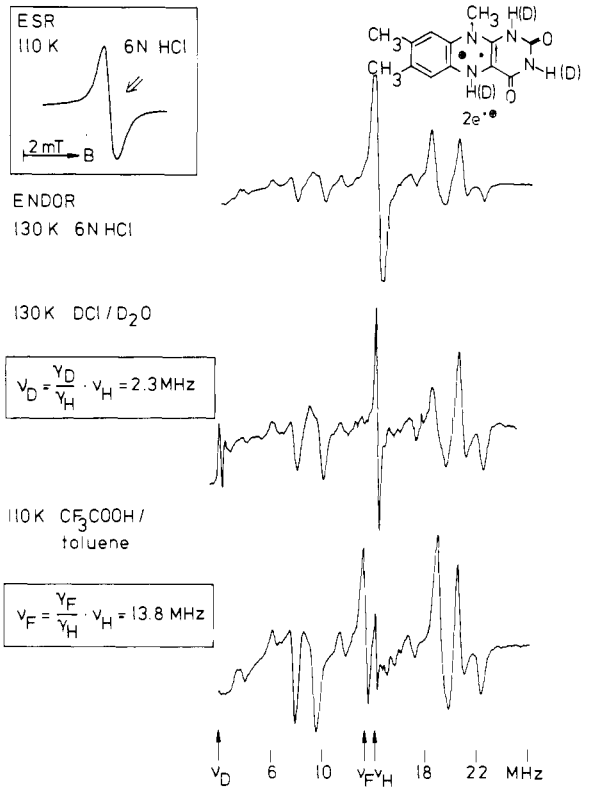

Figure 5. ENDOR spectra in disordered solids of lumiflavin cation radicals. Note the free proton, free deuterium, and free fluorine MATRIX ENDOR signals at their respective free nuclear frequencies.

those belonging to freely rotating methyl groups (see Discussion).

Figure 5 shows the ENDOR spectra of the lumiflavin cation radical taken at 110 K in three different matrices, namely,

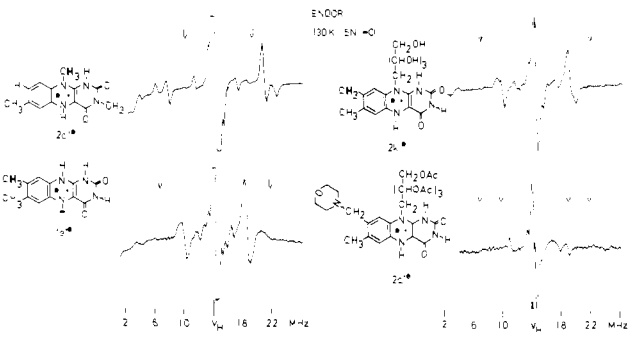

Figure 6. ENDOR spectra in disordered solids of differently substituted isoalloxazine cation radicals. The arrows indicate the ENDOR frequency positions of the substituted (eliminated) methyl groups.

HCl/H_2O, DCl/D_2O, and CF_3COOH/toluene. Apart from the free proton, free deuterium, and free fluorine MATRIX ENDOR signals occurring at the respective free nuclear frequencies, three different methyl group H ENDOR line pairs clearly show up. It is noteworthy that the latter are additionally split (see Discussion). In order to assign the methyl resonances to molecular positions we have compared the ENDOR spectra of the cation radicals of 8-normethyllumiflavin (**2c**$^{+\cdot}$), lumichrome (**1e**$^{+\cdot}$), riboflavin (**2k**$^{+\cdot}$), and 8α-morpholinotetraacetylriboflavin (**2o**$^{+\cdot}$). By inspection of Figure 6 it is clearly seen that the largest splitting has to be assigned to the methyl group in position 10 whereas the second largest one belongs to the 8-methyl group. When a methyl group is substituted, e.g., by ribityl as in vitamin B_2 or by the morpholino group (**2o**$^{+\cdot}$), the corresponding CH_2– group is not free to rotate; hence, the corresponding ENDOR lines are smeared out. Figure 6 demonstrates that either replacement of methyl to give the normethyl compound or substitution of methyl affects the solid-state ENDOR spectrum very similarly. The ENDOR spectrum of the 7-normethyllumiflavin (**2d**$^{+\cdot}$) cation radical supports the assignment of the ENDOR line pair around the proton MATRIX

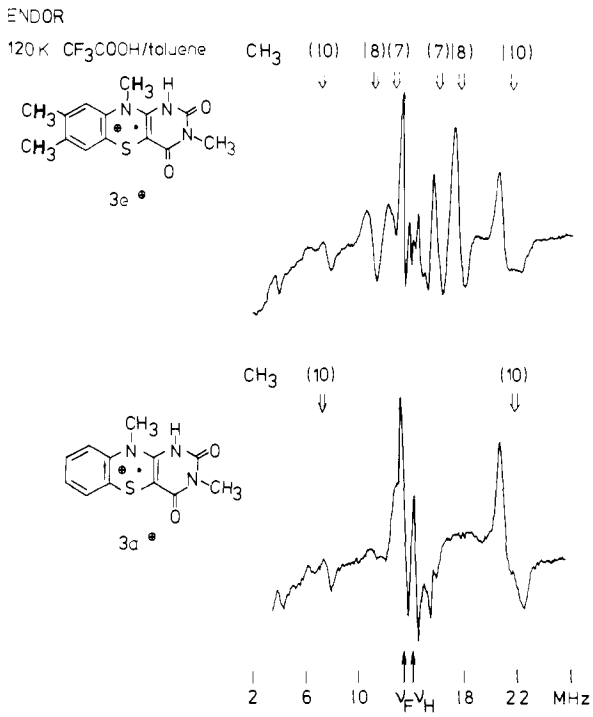

Figure 7. ENDOR spectra in disordered solids of a thiaisoalloxazine and a 7,8-dinormethylthiaisoalloxazine cation radical.

signal to 7-methyl. As can be seen in Figure 5 another ENDOR line pair, e.g., of $2e^{+\cdot}$, referring to a hfsc of about 5 MHz shows up in the spectra. Since these lines proved to be absent in the spectrum of $2h^{+\cdot}$ in DCl as the solvent, these lines apparently can be assigned to the proton in position 6α (cf. Table IV).

The spin density redistribution caused by replacement of N in the 5 position by sulfur—already recognized in the fluid solution spectra—is also reflected in the solid-state spectra. Figure 7 shows the powder ENDOR spectra of thiaisoalloxazine cation ($3e^{+\cdot}$) radical and of its 7,8-dinormethyl derivative ($3a^{+\cdot}$) (see Table IV).

Solid-State ENDOR Measurements of Flavoenzymes. Whereas the solid-state ESR spectrum of the OYE radical in Tris buffer at 130 K consists of only one single line, the ENDOR spectrum, with ESR center field setting, clearly shows a proton MATRIX ENDOR signal and two methyl group ENDOR line pairs (see Figure 8). Since the prosthetic group of OYE is known to be FMN, the solid-state ENDOR spectrum of FMN anion radical is also reproduced for comparison (Figure 8). As in the model compound studies, the high-frequency methyl H ENDOR signal is additionally split, which is especially seen in the special TRIPLE spectrum of the OYE radical (see Figure 8). In Figure 9 the ENDOR spectra of the two flavodoxins from *M. elsdenii* and *A. vinelandii* and that of the FMN neutral radical are depicted. In contrast with OYE and the flavodoxins the prosthetic group of methanol oxidase is FAD. Thus, in Figure 10 the ENDOR spectra of methanol oxidase, taken at two different field settings (see Discussion), and that of FAD anion radical are reproduced.

Discussion

Our high-resolution ENDOR experiments on flavin model compounds in fluid solution clearly demonstrate the significant physical and engineering progress of this spectroscopy achieved during the last decade. In fact, we are aware of only one previous paper dealing with fluid solution ENDOR of flavin radicals (metal ion chelates) and only the strongly coupled methyl proton signals could be detected.[6e] In our ENDOR and TRIPLE experiments, however, the complete sets of isotropic proton and nitrogen hfsc's of the flavin and thiaflavin radicals including their signs could be obtained (at least the hfsc's larger than 0.3 MHz for protons and 1 MHz for the nitrogens) (see Table III). As was already pointed out, the hfsc's could unambiguously be assigned to molecular positions by using selectively deuterated and/or substituted derivatives. Substitution of H by CH_3 does not alter the π-spin

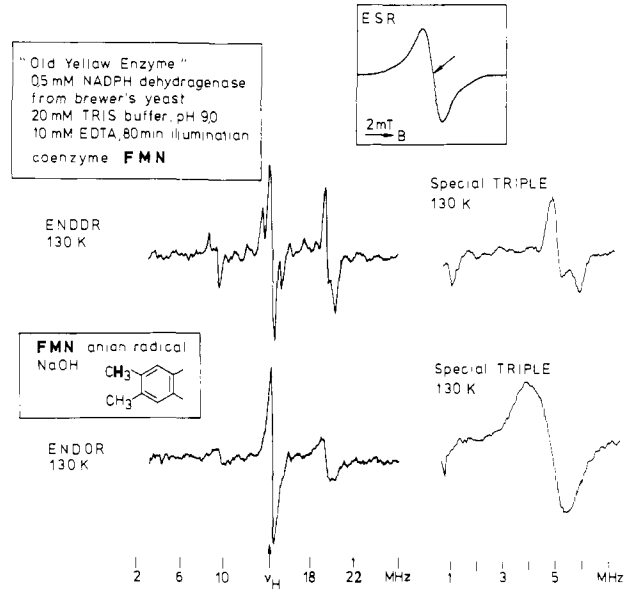

Figure 8. ESR, ENDOR, and special TRIPLE spectra in disordered solids of the radical state of old yellow enzyme and of the FMN anion radical.

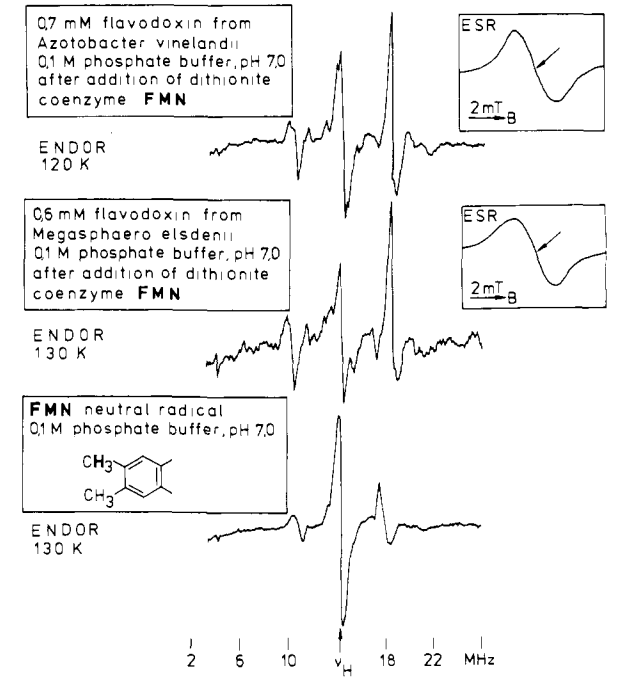

Figure 9. ESR and ENDOR spectra in disordered solids of two flavodoxins and ENDOR spectrum of the FMN neutral radical.

distribution appreciably, and the value of the methyl hfsc increases only slightly. Since the sign of the methyl proton hfsc's is changed as compared to those of the respective protons, this kind of substitution allows assignments of hfsc's to positions where selective deuteration is rather difficult, e.g., in the case of the methyl groups in positions 7 and 8.

The larger hfsc's obtained by ENDOR compare well with the data elucidated from ESR by Müller et al.[29] using a sophisticated computer-simulation program for the analysis of the moderately resolved ESR spectra. On the other hand, the ENDOR technique proved to be superior as regards determination and assignments of the smaller hfsc's. Actually, earlier assignments of the hfsc of 0.3 MHz to position 9 of $2e^{+\cdot}$[29] and of that of position 7 of

(29) Müller, F.; Grande, H. J.; Harding, L. J.; Dunham, W. R.; Visser, A. J. W. G.; Reinders, J. H.; Hemmerich, P.; Ehrenberg, A. *Eur. J. Biochem.* **1981**, *116*, 17.

Table IV. Anisotropic and Calculated Isotropic Hyperfine Coupling Constants (MHz)[a] in Disordered Solids

compd no.	$a_{CH_3}^{H} \times (10)_\perp$	$a_{CH_3}^{H} \times (10)_\parallel$	$a_{CH_3}^{H} \times (10)_{iso}$	$a_{CH_3}^{H} \times (8)_\perp$	$a_{CH_3}^{H} \times (8)_\parallel$	$a_{CH_3}^{H} \times (8)_{iso}$	$a_{CH_3}^{H} \times (7)_\perp$	$a_{CH_3}^{H} \times (7)_\parallel$	$a_{CH_3}^{H} \times (7)_{iso}$	$a^{H} \times (6)_{iso}$	solvent
$1b^{+\cdot}$				9.9	8.3	8.8				5.7	DCl
$1c^{+\cdot}$										5.1	HCl
$1d^{+\cdot}$				9.4	8.1	8.5				5.5	DCl
$1e^{+\cdot}$				9.8	8.6	9.0			1.8	4.8	HCl
$1h^{+\cdot}$				9.9	8.6	9.0			1.8		DCl
$2a^{+\cdot}$	16.6	13.2	14.3							6.1	DCl
$2b^{+\cdot}$	16.2	12.6	13.8	10.1	8.4	9.0				6.4	HCl
$\mathbf{2c}^{+\cdot}$	16.7	13.0	14.2						2.0	5.7	HCl
$2d^{+\cdot}$	15.9	12.8	13.8	10.2	8.0	8.7					HCl
$2f^{+\cdot}$	16.6	13.0	14.2	10.7	9.0	9.6			1.9	5.5	HCl
$2f^{+\cdot}$	16.4	13.0	14.1	11.4	9.8	10.3				5.4	CF_3COOH/toluene
$\mathbf{2f}^{+\cdot}$	16.5	13.2	14.3	10.8	9.4	9.9				5.4	CCl_3COOH/toluene
$2h^{+\cdot}$	16.5	13.1	14.2	10.5	8.9	9.4			1.9		DCl
$2i^{+\cdot}$	2.5 (D)	2.1 (D)	2.2 (D)	10.5	8.7	9.3				5.4	DCl
$\mathbf{2k}^{+\cdot}$				10.9	9.2	9.8			1.9	5.6	HCl
$\mathbf{2l}^{+\cdot}$				10.7	9.0	9.6			1.9	5.5	HCl
$2m^{+\cdot}$				11.7	10.2	10.7			1.5	5.5	CF_3COOH/toluene
$2o^{+\cdot}$										6.6	HCl
$2n^{\cdot}$	14.7	11.5	12.5	9.0	7.8	8.2				5.6	$CHCl_3$
$\mathbf{2n}^{\cdot c}$	13.6	10.7	11.7	8.3	6.7	7.2				5.2	$CHCl_3$
$\mathbf{2n}^{-\cdot}$	12.4	9.4	10.4	10.9	10.3	10.5			1.6	3.7	THF
$\mathbf{2l}^{\cdot}$				9.1	7.0	7.7				2.2	pH 7
$\mathbf{2l}^{-\cdot}$				12.7	9.9	10.8				3.4	0.1 N NaOH
$\mathbf{2m}^{\cdot}$				9.7	7.4	8.2					pH 5.5
$\mathbf{2m}^{-\cdot}$				12.0	10.6	11.5					0.1 N NaOH
Fl[d]				9.5	7.7	8.3				5.5	pH 7.0
Fl[e]				9.5	8.0	8.5			1.6	5.6	pH 7.0
OYE[f]				12.3	10.3	10.9			1.8	3.7	pH 9.0
MO[g]				11.9	9.9	10.6				2.1	pH 7.5
MO[h]				11.7	10.0	10.6				2.1	pH 7.5
				12.4	10.5	11.2					
$3a^{+\cdot}$	16.7	13.4	14.5								CF_3COOH
$3b^{+\cdot}$	16.2	13.4	14.3	7.6	6.3	6.7					CF_3COOH
$3d^{+\cdot}$	16.2	13.3	14.3	7.3	6.0	6.4					CF_3COOH
$\mathbf{3e}^{+\cdot}$	16.4	13.1	14.2	8.0	6.3	6.9	4.5	2.9	3.4		CF_3COOH/toluene

[a] All hfsc's are measured by ENDOR and are accurate within ±0.3 MHz. Temperature range 110–150 K. [b] Calculated by using $a_{CH_3}^{H} \times (10)_\perp$ and $a_{CH_3}^{H}(10)_\parallel$. cf. ref 7c. [c] Proton hfsc's of CH_3 in position 5: 22.4/20.7/21.3. [d] Flavodoxin from *A. vinelandii*. [e] Flavodoxin from *M. elsdenii*. [f] NADPH dehydrogenase (OYE). [g] Methanol oxidase from *C. boidinii*. [h] Methanol oxidase after addition of H_2NOH; see the text.

$\mathbf{3e}^{+\cdot}$[5b] have to be revised (see Table III). In agreement with earlier ESR results[29] our ENDOR studies reveal that in flavin radicals the unpaired spin density is essentially localized on the benzopyrazine moiety. The small hfsc's obtained for the methyl protons in 3-methyl-substituted flavin and thiaflavin radicals indicate some spin density to be present in the pyrimidine part of the heterocyclic systems (for assignment, see Figures 3 and 4). The largest hfsc's have to be attributed to the nitrogens in positions 5 and 10 and to the 8-methyl protons. The hfsc of the latter turned out to be very sensitive to substitution of the isoalloxazine ring, see, e.g., $\mathbf{2d}^{+\cdot}$. Substitution of either the 8-methyl (to obtain an 8α-morpholino-substituted compound) or the 10-methyl group (riboflavin) significantly decreases the respective proton (now $-CH_2-$) hfsc's (Table III). This fact can be understood in the framework of the hyperconjugation model, implying a strong conformational dependence of the hfsc's of these protons.[30] For the largest side chain in flavoenzymes, i.e., FAD, two different hfsc's are obtained for the two β-protons at position 10. This is in contrast to the other coenzymes (FMN, riboflavin). The former effect is caused by the size of the side chain and its pronounced hindered rotation.

As can be seen from Table III, substitution of nitrogen in the 5 position by sulfur ("thiaflavin radicals") causes a considerable redistribution of the spin density within the benzene fragment. Fenner et al.[5b] were the first to measure hfsc's of the thiaflavin radicals and assigned them to molecular positions similar to the flavin radicals. Deuteration and methyl substitution of the thiaflavin system show, however, that the spin density in the benzenoid part has to be assigned differently. Whereas the hfsc's of positions 7 and 8 have the largest values, that of position 6 is only very small (Table III). It has been noted previously that substitution of N by S, e.g., in the phenazinium cation radical to form phenothiazinium cation radical, affects the spin density distribution.[31] As in the case of the phenazinium/phenothiazinium cation systems, in the thiaflavin radicals the spin density at the corresponding position 7 is increased as compared to that in the flavin radicals. Moreover, the spin density in the pyrimidine part of the thiaflavin radical is somewhat larger than in the flavin radical. These differences are caused by the electronic properties of the sulfur.

In either group, i.e., the flavin and the thiaflavin series, the hfsc's of the cation radicals are quite different from those of the neutral radicals. Deprotonation of the cation radicals to generate the neutral radicals decreases most of the hfsc's. Regarding the flavins it has to be pointed out, however, that generation of stable neutral flavin radicals requires alkylation at N(5) position. Thus, replacement of a proton by, e.g., methyl is at least partly responsible for the changes of the hfsc's.

It has been reported that ESR spectra from flavoenzymes exhibit features from nonaveraged hyperfine anisotropy even in fluid solution.[6e] Obviously, molecular tumbling of the protein is not fast enough at room temperature in water. Assuming a molecular weight (M_r) of 10000 (100000), a rotational correlation time τ_R of 3 (30) ns is estimated for an aqueous solution at 25 °C by using $\tau_R = (3 \times 10^{-13})M_r$ (s).[32] Thus, the Redfield condition[33]

$$\langle \mathcal{H}(t) \rangle \tau_R / \hbar < 1$$

(30) Broser, W.; Kurreck, H.; Oestreich-Janzen, S.; Schlömp, G.; Fey, H.-J.; Kirste, B. *Tetrahedron* **1979**, *35*, 1159, and references cited therein.

(31) Sullivan, P. D.; Bolton, J. R. *J. Magn. Reson.* **1969**, *1*, 356.
(32) Chasteen, N. D.; Francavilla, J. *J. Phys. Chem.* **1976**, *80*, 867.

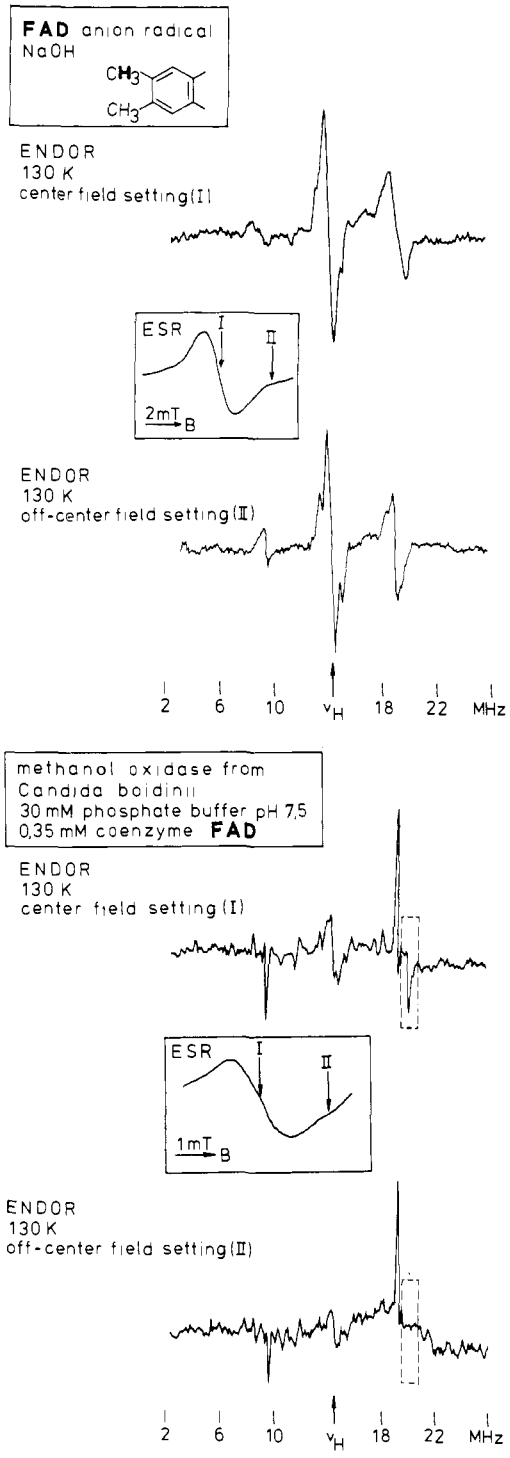

Figure 10. ESR and ENDOR spectra in disordered solids of methanol oxidase and the FAD anion radical at two different field settings.

for fast motion is only valid for nuclei with anisotropic hyperfine couplings <50 (<5) MHz. From simulations of solid-state ESR spectra of flavin radicals, it is known[4b] that the components of the nitrogen-14 hyperfine tensor are

$$A_{\parallel} = 2.5a_{N(iso)}$$

$$A_{\perp} = 0.25a_{N(iso)}$$

Since $a_{N(iso)}$ is ca. 20 MHz for N in position 5 the anisotropy of this hfsc is expected not to be averaged out in solution spectra of flavoenzymes. On the other hand, increased temperatures and/or different solvents with lower viscosity cannot be used for enzymes, leading to the destruction of the protein structure. Hence, normal, i.e., "isotropic", solution ENDOR spectra cannot be expected for all nuclei in flavoenzymes.[34] Furthermore, up to now it is still an open question whether the relaxation conditions of the flavoenzymes at room temperature will allow detection of ENDOR signals at all, that is, with a sufficient signal to noise ratio. Therefore, to date the most promising approach is offered by ENDOR in frozen solution since appropriate single crystals of flavoenzymes are not easy to obtain.

MATRIX ENDOR. In the ENDOR measurements of the flavin radicals in disordered solids, the most pronounced resonances are those occurring at the free nuclear frequencies ("MATRIX ENDOR") and those of the methyl protons. MATRIX ENDOR is known to originate from purely dipolar hyperfine interactions of the unpaired electron with magnetic nuclei of the matrix at distances within roughly 0.6 nm (6 Å).[3h] This resonance is found at the free nuclear frequency corresponding to the magnitude of the external magnetic field. Depending on the matrix used, free proton, free deuterium, and free fluorine ENDOR lines clearly show up in the ENDOR spectra (see Figure 5). Interestingly, the ENDOR line at the free proton frequency is found in all matrices used, even in the DCl/D_2O matrix isotopically enriched by more than 99%. Thus, it can be concluded that this line may be due to hyperfine interactions with nearby diamagnetic flavin molecules. Consequently, in HCl/H_2O the ENDOR signal at the free proton frequency represents a superposition of both types of resonances. The fluorine MATRIX ENDOR obtained here, e.g., with the lumiflavin cation radical in trifluoroacetic acid/toluene has previously been observed for quite different species, e.g., di-*tert*-butyl nitroxide in the 1*H*,1*H*-heptafluoro-1-butanol matrix at 48 K.[35] In our experiments it is still an open question whether the hyperfine coupled fluorine nuclei are part of an ion pair consisting of the flavin cation and the trifluoroacetate anion or belong to a trifluoroacetic acid molecule in the solvation shell. It has to be mentioned, however, that, because of hydrogen bridging, even the possibility of a proper distinction between counter anion and solvation shell is rather speculative. In order to confirm that this resonance originates from fluorine hyperfine interactions we have repeated this experiment by using trichloroacetic acid instead of trifluoroacetic acid. The same ENDOR spectrum was obtained except for the absence of the fluorine MATRIX ENDOR signal.

When the intensity of the free proton frequency line is compared with that of the methyl protons, there is no doubt that the free coenzymes show a much more intense MATRIX ENDOR line than the native enzymes (cf. Figures 8–10). In fact, a very small MATRIX ENDOR signal is found for methanol oxidase. The reason for this finding may tentatively be explained by the assumption that the flavin radical is imbedded within a hydrophobic part of the protein. Hence, the "hyperfine active" surrounding of the radical is much less accessible to the proton-rich water molecules than in the protein-free species. Similar conclusions have previously been drawn from MATRIX ENDOR measurements of OYE and of the flavodoxins.[6d]

MATRIX ENDOR studies[36] of the tritolylmethyl radical in polycrystalline and glassy phases of toluene have shown that the amount of molecular motion is quite different in these different phases, thereby affecting the intensity of the MATRIX ENDOR signal. Thus MATRIX ENDOR can be used to probe the surroundings of radical species, vide infra.

Methyl Proton ENDOR in Disordered Solids. As was already pointed out under Results, solid-state ENDOR allows unambiguous identification of unsubstituted, i.e., freely rotating, methyl groups. In accordance with previous investigations[37] our flavo-

(33) Redfield, A. G. *Adv. Magn. Reson.* **1965**, *1*, 1.

(34) Such spectra were recently obtained from chlorophyll/protein complexes (reaction centers) where the observed chlorophyll cation shows fluid solution ENDOR signals of nuclei bearing only small hyperfine anisotropy: Hoff, A. J.; Lendzian, F.; Möbius, K.; Lubitz, W. *Chem. Phys. Lett.* **1982**, *85*, 3.

(35) Schwartz, R. N.; Bowman, M. K.; Kevan, L., unpublished, cited in ref 7c.

(36) Hyde, J. S.; Rist, G. H.; Eriksson, L. E. G. *J. Phys. Chem.* **1968**, *72*, 4269.

(37) See ref 17 and 7c and references cited therein.

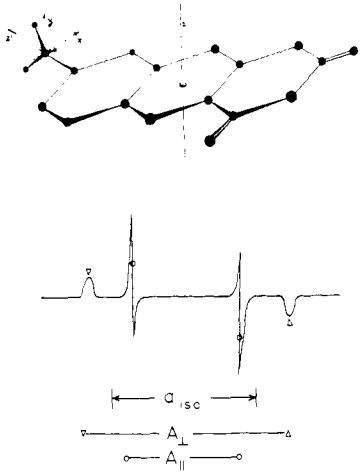

Figure 11. Structure of the isoalloxazine ring system and schematic drawing of the powder ENDOR spectrum of a freely rotating methyl group. Resonance positions of the $A_{\parallel}$ components were taken according to the procedure given by Wasserman et al.[40]

enzyme ENDOR studies indicate that in OYE, in the flavodoxins, and in methanol oxidase the apoprotein is noncovalently linked to the prosthetic group via 8-methyl (see Figures 8–10). The additional splittings, i.e., the resolved components of the anisotropic hyperfine tensors of the methyl group protons in the powder ENDOR spectra, are no doubt of the greatest importance in these studies and thus worthwhile of being discussed in more detail. In frozen solutions of free flavin or flavoenzyme radicals, the dominant anisotropic contribution is expected from the ^{14}N hfsc's in positions 5 and 10. Furthermore, the g anisotropy is small, i.e., $\Delta g = 0.0015$.[6b] This results in a superposition of hyperfine components belonging to different orientations in the center part of the ESR spectrum. Performing ENDOR experiments by desaturating this region of the ESR spectrum yields a powder ENDOR pattern. The outer parts of the ESR spectrum, however, predominantly arise from molecules that have the ^{14}N M_I values either +1 or −1 and therefore have their molecular plane perpendicular to the magnetic field.[6b] Hence, by desaturation of the spectral wings of the ESR spectrum, single-crystal-like ENDOR spectra are expected. The degree of orientational selection by double-resonance techniques is, of course, limited by the separation of the respective components in the ESR spectrum. In the case of X-band powder ESR spectra of "immobilized" flavins, this resolution is rather poor and real single-crystal-like ENDOR spectra are difficult to obtain, vide infra.

The possible types of ENDOR spectra of disordered solids have exhaustively been discussed by Kevan and Kispert.[7c] In single-crystal-like ENDOR spectra only those components of the proton hyperfine tensors can be detected that have their axis parallel to the respective perpendicular component of the ^{14}N hyperfine tensor. In the case of the methyl groups this is the out of plane (z) component A [i.e., parallel to $A_{zz}(^{14}N)$] (see Figure 11). In the powder ENDOR spectra an average of all orientations of the hyperfine tensors for each individual nucleus is measured. Thus, the ENDOR spectrum for such a nucleus extends over the whole range of the hyperfine values, with some buildup of intensity at the principal values of the hyperfine tensor. For α-protons, e.g., in position 5 of the isoalloxazine system, however, the resonance region is smeared out over a large frequency range, namely, from $0.5a$ to $1.5a$ with spectral features at $0.5a$, a, and $1.5a$. Normally it will be very difficult to detect these resonances at all.[6b] In our experiments these resonances and those of ^{14}N could not be clearly identified up to now except for the proton in position 6α (see, e.g., Figures 5 and 6).[38]

The situation is quite different when dealing with the three protons of a freely rotating methyl group. These protons are equivalent on the ESR time scale, the hyperfine tensor is axially symmetric, and the nuclear anisotropy is less than 10% of the respective isotropic hfsc a.[4b] A buildup of intensity of the ENDOR absorption is obtained at ca. $0.9a$ and $1.1a$, i.e., close to a_{iso}. With respect to ENDOR intensity this is the most favorable situation for spectra of disordered solids. A convenient way of improving the resolution of these powder ENDOR patterns is by frequency modulating the rf field followed by phase-sensitive detection, resulting in a first derivative of the ENDOR signal vs. the rf frequency. This technique (see, e.g., Figures 5–7) is used in our experiments, and often both components of the methyl hyperfine tensor could be measured (the patterns are depicted schematically in Figure 11). In fact, the freely rotating methyl groups in the 7, 8, and 10 positions of free flavin and thiaflavin radicals give rise to intense ENDOR signals. The anisotropic hyperfine data allow determination of the respective isotropic hfsc's following the procedure described previously.[7c] As can be seen from Tables III and IV the calculated isotropic hfsc's compare well with those obtained from the fluid solution measurements. Thus, it can be concluded that freezing of the solution does not affect the spin density distributions significantly.

In agreement with the discussion given above, the powder ENDOR line pattern of methanol oxidase exhibits a significant dependence on the external field setting (see Figure 10). If the external field is set at the center of the ESR spectrum—this is the usual field setting in an ENDOR experiment—the various methyl components are recorded nonselectively and a powder-type ENDOR spectrum is obtained. Off-center field setting at a wing position of the ESR spectrum represents a fairly discrete orientation of the molecules with respect to the external magnetic field. Thus, a single-crystal-like ENDOR spectrum is obtained. Actually only *one* high-frequency signal is observed for the 8-methyl group. The largest anisotropic hyperfine component of a methyl group is known to be along the C–C bond direction.[6e] Since this ENDOR component is no longer seen in the off-center field setting experiment, it can be concluded that the C–C bond direction of 8-methyl is perpendicular to the main hyperfine components of the nitrogens in positions 5 and 10. Hence, the isoalloxazine ring system must be fairly coplanar in the radical state. If the heterocyclic system were nonplanar, for example, in a kind of butterfly conformation, there would be no reasonable explanation for the significant dependence of the methyl proton ENDOR signals on the field setting.

Besides ENDOR intensities, the most important problem in solid-state spectra is resolution. In the case of single-crystal-like spectra quite narrow lines can be obtained. Larger line widths are expected for powder-type spectra due to anisotropic broadening. Furthermore, each individual hyperfine component—for a certain orientation—is additionally broadened by environmental effects, i.e., by the range of crystal field distributions in the polycrystalline host lattice. Pronounced effects are expected for polar noninert hosts that are able to interact with the guest molecules, thereby changing their magnetic parameters and increasing the number of sites. In this respect, water is expected to be one of the poorest solvents due to its high polarity, its ability to form hydrogen bonds, and the formation of a variety of crystalline forms. Water is, however, the required solvent in the studies of biological systems.

In the powder ENDOR spectra obtained from different flavin model compounds (Figures 5–7), FMN (Figures 8 and 9), and FAD (Figure 10), the line widths of the radicals in frozen water are indeed very large (~300 kHz) and the resolution is low. A similar situation is met with the flavodoxins, in which the flavin mobility is known to be small[41] and the complexation is very strong;[16] the active site seems to be accessible to water. In the

(38) In the case of ^{14}N ENDOR an additional complication arises from the nuclear quadrupole interaction that splits the ENDOR lines and thereby increases the range of resonances and increases the overall intensity. On the other hand, detection of ^{14}N ENDOR in disordered solids should, in principle, be possible in the studies of flavin radicals since it was already described for other systems.[39]

(39) Box, H. C.; Freund, H. G.; Budzinski, E. E. *J. Chem. Phys.* **1967**, *46*, 4470.
(40) Wasserman, E.; Snyder, W. C.; Yager, W. A. *J. Chem. Phys.* **1964**, *41*, 1763.
(41) Moonen, C. T. W.; Müller, F. *Eur. J. Biochem.* **1983**, *133*, 463.

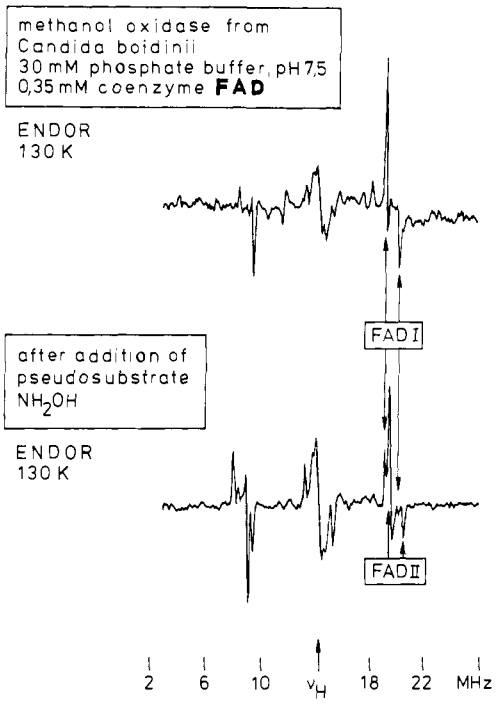

Figure 12. ENDOR spectra in disordered solids of methanol oxidase before and after addition of the pseudosubstrate NH_2OH; see the text.

frozen state this results in a larger ENDOR line width (~300 kHz) for the 8-methyl resonances (Figure 9). The water molecules present in the immediate surrounding of the prosthetic group and the restricted motion result in a relatively intense MATRIX ENDOR signal, supporting the above assumptions. A similar situation is found for OYE (see Figure 8). Interestingly, the radical in methanol oxidase exhibits a quite different behavior; i.e., sharp ENDOR resonances of only ~100 kHz are obtained (Figures 10 and 12). This could indicate that the prosthetic group of this enzyme possesses a larger internal mobility than those of the other flavoproteins studied. It may be assumed that this motion averages specific local interactions, resulting in smaller effective line widths. Furthermore, the microenvironment of the FAD seems to be very hydrophobic. To summarize both these effects, the absence of water and the molecular motion lead to weak MATRIX ENDOR lines and to very narrow line widths for the 8-methyl ENDOR resonances. Recently it has been noted that the different mobilities of the prosthetic groups may be correlated with the enzyme activities.[42] We believe that MATRIX ENDOR and line widths ENDOR studies may contribute to a better understanding of these correlations.

Methanol oxidase isolated from the yeast named *C. boidinii* has a molecular weight of about 600 000 and consists of eight subunits. Each subunit binds one FAD prosthetic group. In the studies of this enzyme the redox stoichiometry turned out to be strictly *two electrons*. Thus, in principle, no radical state is involved during turnover of the enzyme. But on the other hand, a free radical can be detected by ESR in the isolated enzyme, which is stable toward oxygen.[26] The radical concentration was determined to be about 30% of the total amount of FAD present. It has been suggested that the radical might serve as a means for activity regulation.[43] It is, however, to be noted that this is a unique and not yet understood mechanism. The reason for this stability is still unknown. In Figure 10 the ENDOR spectra of methanol oxidase recorded at two different ESR field settings and that of FAD anion radical are reproduced, vide supra. Recently Hemmerich et al.[26] reported that addition of hydroxylamine as a sort of "pseudosubstrate" to methanol oxidase increases the radical concentration from 30 to about 80%. In contrast with their results obtained from UV and ESR studies, our ENDOR experiments unambiguously demonstrate that after addition of hydroxylamine a *different* FAD radical is generated in the enzyme; i.e., two different FAD radical species can be discriminated in this sample (Figure 12). Since the complex flavoenzyme molecule possesses eight FAD groups it is still an open question whether the two types of radicals belong to the same molecule or not. The different spin density distributions may either be caused by different interactions with the apoprotein or by a kind of complexation with the hydroxylamine. Obviously, the radical species present in the starting material remains unaffected by the addition of the hydroxylamine.

(42) Visser, A. J. W. G.; Penners, N. H. G.; Müller, F. "Mobility and Recognition in Cell Biology"; W. de Gruyter: Berlin, 1983; p 137.
(43) Mincey, T.; Tayrien, G.; Mildran, A. S.; Abeles, R. H. *Proc. Natl. Acad. Sci. U.S.A.* **1980**, *77*, 7099.

Conclusion

It has been demonstrated that high-resolution ENDOR and TRIPLE resonance spectroscopy including H, D, and ^{14}N ENDOR can be successfully applied to investigate flavin model compounds. In contrast with conventional ESR the complete sets of hfsc's including their signs can be deduced and assigned to molecular positions. Comparison of polycrystalline and single-crystal-like ENDOR spectra can give information of the geometries of the flavin radicals, e.g., of the planarity of the π-system. From MATRIX ENDOR studies valuable information about molecular motions can be obtained. The type of flavoenzyme radical, i.e., cationic, anionic, or neutral state, can be determined. This technique can be applied to native flavoenzymes, and the type of binding between the apoprotein and the prosthetic group can be evaluated. If more than one flavin (FMN or FAD) is present in the enzyme in a different environment ("site") or state, this difference also shows up in a well-resolved ENDOR spectrum.

There is good evidence that anionic and neutral flavin radicals in flavoenzymes play an important role as intermediates in flavoenzyme catalysis. It is challenging to test such processes by reactions with pseudosubstrates. If a long-lived radical is generated, it should be detectable by ESR and ENDOR. It is no doubt the most demanding experiment in this field to perform fluid solution ENDOR of native enzymes under physiological conditions, i.e., aqueous solutions at room temperature. Further work in this very attractive direction is in progress.

Acknowledgment. We thank Prof. H. Fenner and Dr. R. Grauert, Freie Universität Berlin, for supplying us with some thiaflavins. H.K. and P.M.H.K. gratefully acknowledge financial support by the Deutsche Forschungsgemeinschaft (H.K., Ku-505/1-1,1-2; P.M.H.K., Kr 451/8-4) and Fonds der Chemischen Industrie. F.M. acknowledges financial support by the Netherlands Foundation of Chemical Research (S.O.N.) and the Netherlands Organisation for the Advancement for Pure Research (Z.W.O.).

Registry No. **1a**, 490-59-5; **1b**, 58137-51-2; **1c**, 58010-90-5; **1c**, 58010-90-5; **1d**, 88200-69-5; **1e**, 1086-80-2; **1f**, 33174-44-6; **1g**, 88200-70-8; **1h**, 88200-71-9; **2a**, 4074-59-3; **2b**, 62738-33-4; **2c**, 58537-70-5; **2d**, 88200-72-0; **2e**, 1088-56-8; **2f**, 18636-32-3; **2g**, 72184-37-3; **2h**, 88200-73-1; **2i**, 88200-74-2; **2j**, 88200-75-3; **2k**, 83-88-5; **2l**, 146-17-8; **2m**, 146-14-5; **2n**, 74178-39-5; **2o**, 57454-83-8; **2p**, 752-13-6; **3a**, 67236-71-9; **3b**, 88200-76-4; **3c**, 88200-77-5; **3d**, 88200-78-6; **3e**, 70239-38-2; **3f**, 88200-79-7; **3g**, 88200-80-0; **3h**, 79108-69-3; 3,3′-dimethyl-6-(phenylamino)-2,4-(1*H*,3*H*)-pyrimidinedione, 58137-46-5; 3,4′-dimethyl-6-(phenylamino)-2,4-(1*H*,3*H*)-pyrimidinedione, 76896-60-1; 3,3′,5′-trimethyl-6-(phenylamino)-2,4-(1*H*,3*H*)-pyrimidinedione, 88200-81-1; 3,3′,*N*′-trimethyl-6-(phenylamino)-2,4-(1*H*,3*H*)-pyrimidinedione, 88200-82-2; 3,4′,*N*′-trimethyl-6-(phenylamino)-2,4-(1*H*,3*H*)-pyrimidinedione, 88200-83-3; 3,3′,5′,*N*′-tetramethyl-6-(phenylamino)-2,4-(1*H*,3*H*)-pyrimidinedione, 88200-84-4; 3,3′-dimethyl-2′,6′-dideuterio-6-(phenylamino)-2,4-(1*H*,3*H*)-pyrimidinedione, 88200-85-5; 3,3′,4′-trimethyl-2′,5′,6′-trideuterio-6-(phenylamino)-2,4-(1*H*,3*H*)-pyrimidinedione, 88200-86-6; 3,3′,4′,*N*′-tetramethyl-2′,6′-dideuterio-6-(phenylamino)-2,4-(1*H*,3*H*)-pyrimidinedione, 88200-87-7; 3,3′,4′,*N*′-tetramethyl-2′,5′,6′-trideuterio-6-(phenylamino)-2,4-(1*H*,3*H*)-pyrimidinedione, 88200-88-8; 3,3′,4′-trimethyl-*N*′-trideuteriomethyl-2′,5′,6′-trideuterio-6-(phenylamino)-2,4-(1*H*,3*H*)-pyrimidinedione, 88200-89-9; NADPH dehydrogenase, 9001-68-7; methanol oxidase, 56379-53-4.